Modifications at the C-Terminus To Improve Pyrrole−Imidazole Polyamide Activity in Cell Culture

Claire S. Jacobs and Peter B. Dervan*

Division of Chemistry and Chemical Engineering, The California Institute of Technology, 1200 E. California Boulevard, Mail Code 164-30, Pasadena, California 91125

Pyrrole−imidazole (Py-Im) hairpin polyamides are a class of small molecule DNA minor groove binding compounds that have been shown to modulate endogenous gene expression in cell culture. Gene regulation by polyamides requires efficient cellular uptake and nuclear localization properties for candidate compounds. To further optimize Py-Im polyamides for enhanced potency in cell culture, a focused library of polyamides possessing various modifications at the C-terminus was synthesized and tested. Comparison of polyamide biological activity in two cell lines revealed tolerance for structural modifications and agreement in activity trends between cell lines. The use of an oxime linkage between the polyamide and an aromatic functionality on the C-terminus resulted in a ∼20-fold increase in the potency of polyamides targeted to the androgen response element (ARE) in LNCaP cells by measuring AR-activated PSA expression.

Introduction

Small molecules capable of regulating specific endogenous gene expression pathways could find numerous applications in molecular biology and human medicine.[1,2] DNA-binding polyamides comprising *N*-methylimidazole (Im[a]) and *N*-methylpyrrole (Py) are a class of programmable small molecules that bind the minor groove of DNA in a sequence specific fashion and have been employed as regulators of gene expression through DNA-binding and disruption of transcription factor−DNA interfaces.[3] Hairpin polyamides comprise two Im-Py strands linked via an aliphatic linker, with sequence specificity resulting in a programmed fashion from side-by-side heterocyclic amino acid pairings: Im/Py recognizes G·C over C·G; Py/Py is degenerate for A·T and T·A; 3-chlorothiophene N-terminus cap/Py recognizes T·A over A·T.[4−6] Eight-ring Im-Py polyamides have been shown to exhibit specific binding with binding affinities comparable to those of natural DNA-binding transcription factors.[7] Im-Py polyamide regulation of gene expression presumably occurs through either direct steric blockade of transcription factor binding or allosteric modification of DNA topology. While the sequence specificity and DNA-binding affinity of these small molecules are well studied, investigations into their potential therapeutic applications are active areas of investigation. We have recently shown that the biological activity of Im-Py polyamides can be improved via the incorporation of an isophthalic acid (IPA) group at the polyamide C-terminus. We present here further modifications to the hairpin polyamide C-terminus that increase even further their biological activity.[8]

Early gene regulation studies in cell culture relied on fluorescein−polyamide conjugates as cell permeable compounds.[9−13] Subsequent studies aimed at eliminating the fluorescent tag (FITC) utilized quantitative real-time reverse transcriptase polymerase chain reaction (RT-PCR) to measure mRNA levels of an endogenous inducible gene as a biological readout of polyamide nuclear entry and DNA-binding. A focused library of minimized FITC analogues identified a smaller, stable replacement for fluorescein in the form of isophthalic acid (IPA), which rivaled the activity of the original FITC-labeled polyamide in HeLa (cervical cancer) and U251 (glioma) cells.[8] Subsequent work in other cell lines aimed at regulating different target genes has validated this C-terminus modification as a positive contributor to biological activity with negligible detrimental impact on polyamide sequence specificity or binding affinity.[14,15]

The discovery of new moieties that facilitate polyamide cell uptake and nuclear localization for gene regulation studies is an area of keen interest as we aim to enhance further polyamide efficacy as we transition our studies toward animal disease models. The present study investigates the influence of linker, chemical linkage, and target cell line on polyamide nuclear localization utilizing a small library of C-terminus-modified polyamides (Figure 1). Quantitative real-time RT-PCR of relative mRNA expression levels in cells treated with polyamides was used as a measure of biological efficacy and the criterion for ranking members of the polyamide library. Polyamides were targeted either to the vascular endothelial growth factor (VEGF) promoter in U251 (glioma) and LNCaP (prostate) cells or to the prostate specific antigen (PSA) promoter in LNCaP cells (Figure 1B), as these two transcription-factor systems have been exploited for regulating such medically relevant genes by our group.[13−15] Although a variety of structural parameters were evaluated, it was discovered that a C3 aliphatic linker tethered to an aromatic group through an oxime linkage resulted in enhanced polyamide potency. This motif has been employed recently

---

*To whom correspondence should be addressed. Phone: (626) 395-6002. Fax: (626) 683-8753. E-mail: dervan@caltech.edu.

[a] Abbreviations: Im, *N*-methylimidazole; Py, *N*-methylpyrrole; VEGF, vascular endothelial growth factor; HIF, hypoxia-inducible factor; HRE, hypoxia response element; PSA, prostate specific antigen; ARE, androgen response element; IPA, isophthalic acid.
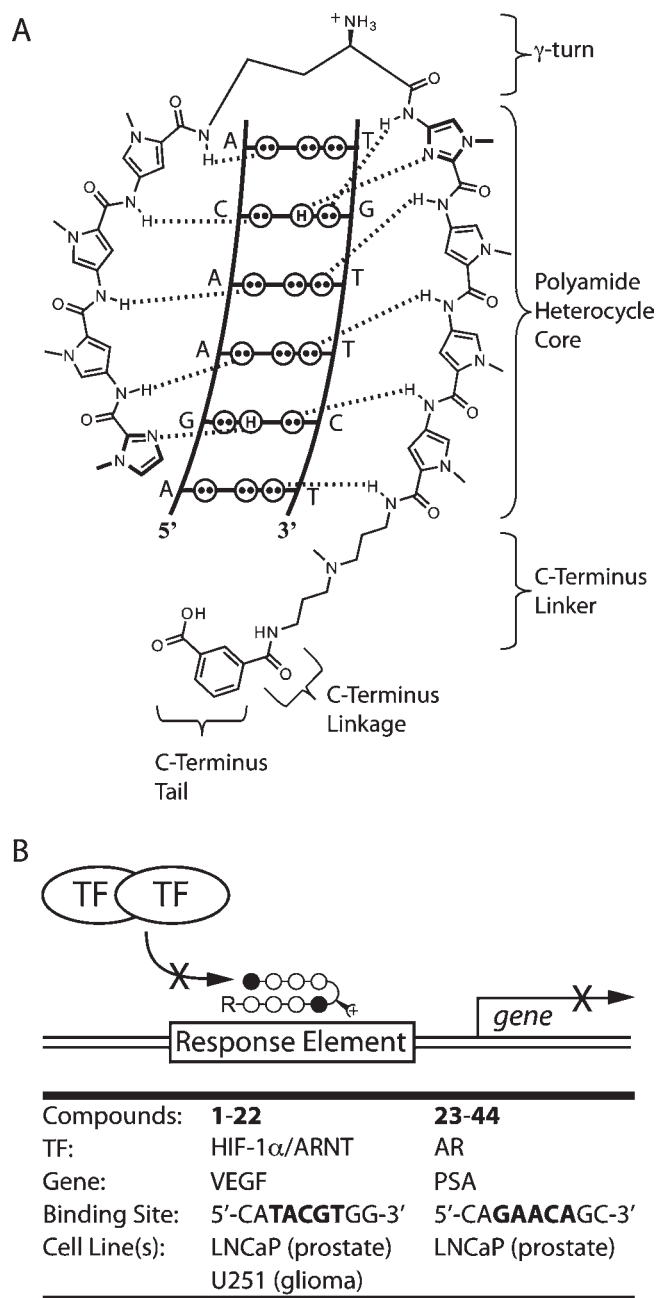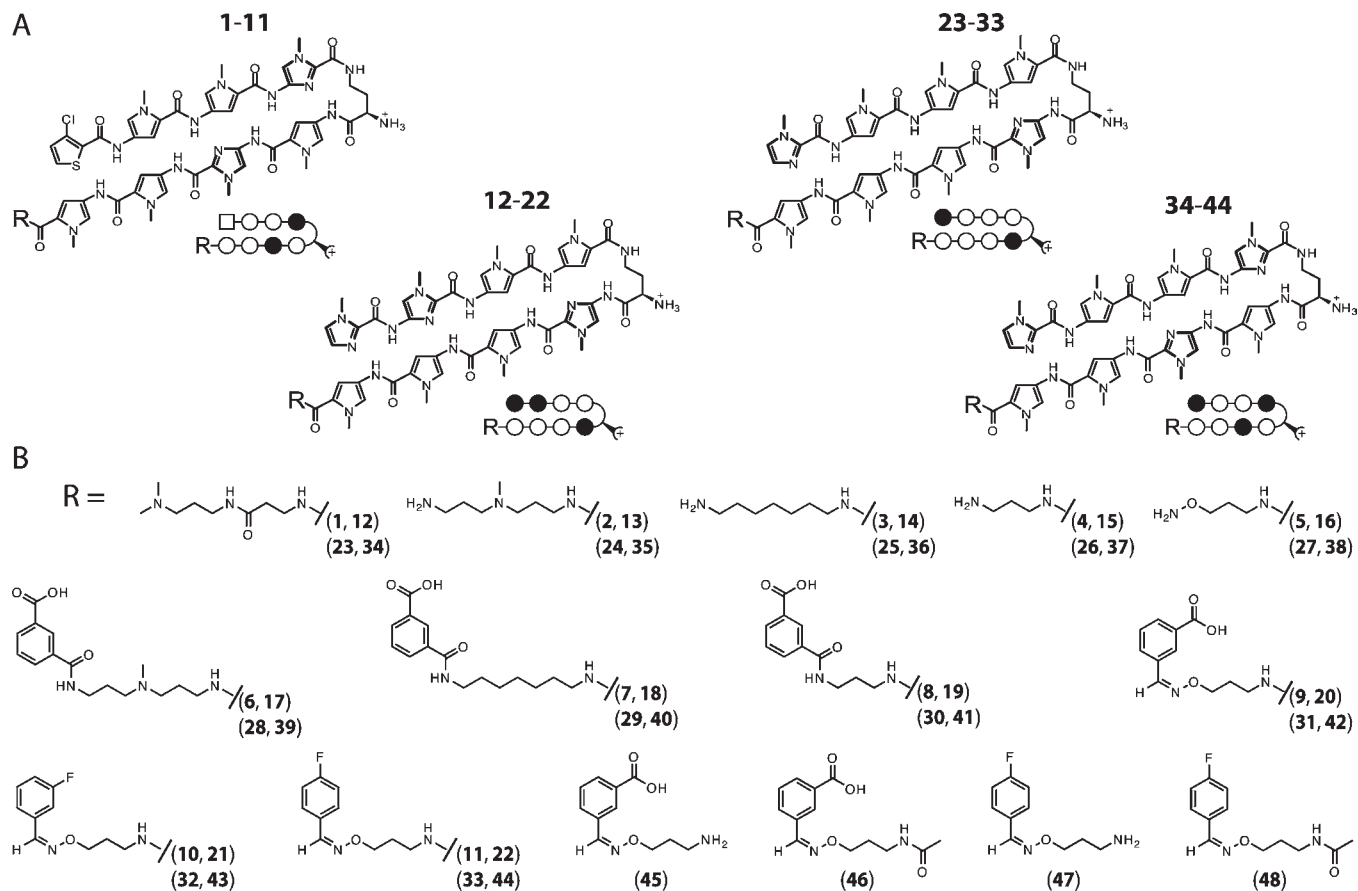
Figure 1. Project overview. (A) Schematic illustration of polyamide−DNA recognition through formation of hydrogen bonds with the floor of the DNA minor groove. The γ-turn, polyamide heterocycle core, C-terminus linker, C-terminus linkage, and C-terminus tail of the polyamide are indicated by braces and labeled for clarity. (B) Schematic illustration of the mechanism by which polyamides affect gene expression. Sequence-specific binding of a polyamide core to a gene response element (RE) blocks transcription factor (TF) binding to the RE, thus blocking up-regulation of gene product expression under inducing conditions. Relative mRNA expression levels under inducing conditions were employed as a biological readout of polyamide cell uptake nuclear localization. Displayed in tabular form are the relevant transcription factors, gene products, DNA RE binding sequence, and cell lines for each set of match and mismatch polyamides.

for the facile ^{18}F-labeling of polyamides for in vivo biodistribution by positron emission tomography.[16] This particular modification, as well as a variety of structural perturbations to the hairpin oligomer C-terminus, is discussed in detail.

Results

Quantitative Real-Time RT-PCR Data for Polyamide-Treated U251 and LNCaP Cells. The biological activity against DFO-induced VEGF expression of HRE-targeted match (**6−11**) and mismatch (**12−22**) eight-ring hairpin polyamides was studied in U251 and LNCaP cell culture and of ARE-targeted match (**28−33**) and mismatch (**39−44**) eight-ring hairpin polyamides against DHT-induced PSA expression in LNCaP cells. A schematic representation of polyamide−DNA binding and an overview of the project are shown in Figure 1. Structures of the polyamide cores and C-terminus are shown in Figure 2, and results for cell culture experiments are shown in Figures 3−6. Polyamides that regulate VEGF expression under hypoxic (inducing) conditions target the hypoxia response element (HRE) 5′-ATACGTG-3′ of the VEGF promoter (compounds **1−11**), and those that target PSA expression following dihydrotesterone (DHT) induction target the androgen response element (ARE) 5′-AGAACAG-3′ of the PSA promoter (compounds **23−33**). For each gene, a set of mismatch control polyamides was included; mismatch polyamides are designed not to bind to the HRE or ARE, though some degree of biological activity is not unexpected, presumably because of off-target effects. The mismatch polyamides for the HRE series are **12−22** (target 5′-WGGWCW-3′ sequences) and for the ARE series are **34−44** (target 5′-WGWCGW-3′ sequences). These compounds are linked either through an amide linkage (**6−8**, **17−19**, **28−30**, and **39−41**) or an oxime linkage (**9−11** and **20−22**, **31−33**, and **42−44**) to a C-terminal tail group. For each linker group, unconjugated free amine control compounds lacking a tail moiety (**2−5** and **13−16**, **24−27**, and **35−38** (match and mismatch polyamides, respectively) were included; because of its historical use and known modest level of biological activity, βDp tail (**1**, **12**, **23**, and **34**) polyamides were included for comparison. Polyamide-untreated uninduced and polyamide-untreated induced conditions were used as controls, and VEGF or PSA mRNA expression levels in treated cells were normalized to those in the untreated, induced controls. Induced and uninduced DMSO-treated control conditions were included to rule out vehicle (DMSO) as the source of relative mRNA expression changes (DMSO concentration of ≤0.1% for all biological experiments).[17] Unless otherwise noted, U251 cells were dosed with polyamides at 1, 0.2, and 0.02 μM, and LNCaP cells were dosed at 10, 2, and 0.2 μM. For both the VEGF and PSA systems, cells were dosed with control unconjugated control polyamides only at the highest concentration.

Biological Activity of HRE-Targeted Polyamides in U251 and LNCaP Cells. The data obtained for the amide-linked HRE series in U251 and LNCaP are shown in parts A and B of Figure 3, respectively. The biological activity measured for **6** is comparable to previously obtained data for **6** at 1 μM in U251 cells.[8,15] The general trend in this cell line indicates that the unconjugated control compounds lacking the IPA tail moiety all exhibited a modest degree of activity but that activity is improved through IPA conjugation. IPA conjugation resulted in a greater increase in activity for compounds bearing the triamine linker than for compounds bearing the C7-linker or C3-linker. The βDp tail was the least active of all C-terminus modifications in this series. In LNCaP cells, the unconjugated controls were more active than in U251 cells, with the unconjugated parent compound **4** as active as IPA

Figure 2. Schematic illustration of the polyamide cores and tail groups employed. (A) At left are given the HRE match (**1−11**) and HRE mismatch (**12−22**) cores employed in U251 and LNCaP cells, and on the right are the ARE match (**23−33**) and ARE mismatch (**34−44**) cores employed in LNCaP cells. Below the chemical structure is a schematic "ball-and-stick" shorthand representation of each core, in which pyrrole (Py) is symbolized by an open circle, imidazole (Im) by a filled circle, and chlorothiophene cap by an open square. (B) The chemical structures of the tail groups "R" for compounds **1−44** are shown. Structures **45−48** are the "coreless" oxime-linked control compounds.

conjugates **6−8**. Conjugation of the IPA tail increased the activity of the triamine and C7-linked compounds, but the difference in activity between unconjugated parents and the IPA derivatives was more modest than in U251 cells. The βDp tail polyamides (**1** and **12**) were more active in LNCaP than U251.

The activity of the HRE oxime-linked series was measured in U251 and LNCaP, and the results are shown in parts A and B of Figure 5, respectively. Compounds **9−11** were active in U251 cells under hypoxic conditions: VEGF mRNA expression was down-regulated ~60% in U251 cells treated with 1 μM **9−11**, which is comparable to the activity of **6** at 1 μM in U251 (Figure 3A). Mismatch polyamide compounds **20−22** were as active in U251 cells as their respective match polyamides **9−11**. In LNCaP cells, compounds **9−11** were also active: VEGF mRNA expression levels measured for cells treated with 10 μM **9−11** were down-regulated ~80%. Mismatch oxime-linked polyamides were significantly active in LNCaP cells.

Biological Activity of ARE-Targeted Polyamides in LNCaP Cells. The relative PSA mRNA levels in LNCaP cells induced with 1 nM DHT and dosed with polyamides **23−44** were measured (Figure 4 and Figure 5C). In the amide series, the unconjugated free amine control compounds **23−26** were more active that the mismatch controls **34−37**. The amide-linked ARE compounds **28−30** were all appreciably active, and a modest linker effect was observed (C7 > C3 > triamine); mismatch

compounds **39−41** were less active than their match mates. The difference in activity between each match **28−30** and respective mismatch **39−41** was greater than measured for VEGF regulation in both U251 and LNCaP.

The activity of the oxime-linked series **31−33** and **42−44** in LNCaP cells was measured at 5, 1, and 0.1 μM, and that for unconjugated controls **27** and **38** was measured at 5 μM; the data are shown in Figure 5C. A significant increase in biological activity was measured for match polyamides **31−33**; all three compounds decreased PSA mRNA levels at 5 μM below untreated, uninduced levels. PSA mRNA levels were reduced to untreated basal levels at 1 μM **31** and **33**. Mismatch polyamides **42−44** were less active than their respective match polyamides **31−33**. The hydroxylamine match control compound **27** down-regulated PSA mRNA levels by ~50%, while the hydroxylamine mismatch compound **38** showed very little activity. LNCaP cells treated with 5 μM **31−33** showed noticeable cytotoxic response upon incubation for 48 h, an effect that was more pronounced for **32** and **33** compared to **31**.

DNA Melting Temperature (T_m). The effect of polyamide binding on 14-mer oligonucleotide melting temperature (T_m) was measured (Table SI 2 in Supporting Information) to confirm that match polyamides possess appreciable DNA binding affinities and thus that lower levels of biological activity are not due to poor DNA binding affinities.[18] T_m measurements require minimal materials and present a rapid
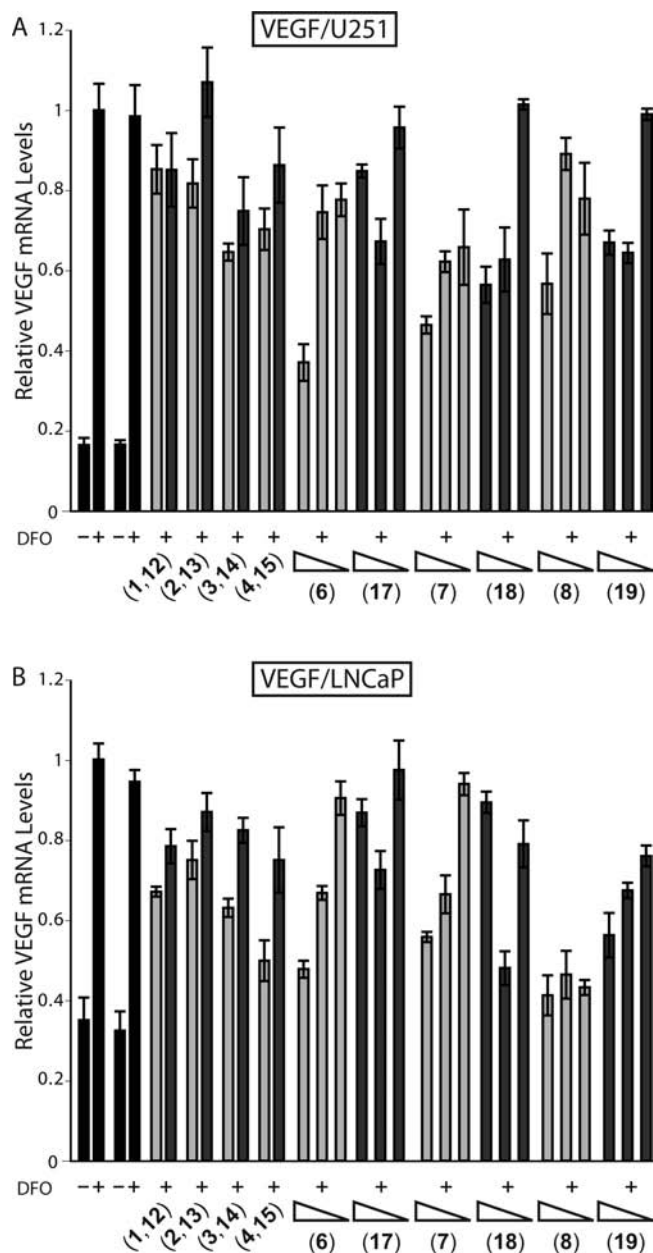
Figure 3. Quantitative real-time RT-PCR data showing the effect of HRE-targeted match compounds **1−4**, **6−8** and their mismatch congeners **12−15**, **17−19** on DFO-induced VEGF expression in cultured cells. Induced and uniduced control conditions are indicated by black bars, match core compounds by light-gray bars, and mismatch core compounds by dark-gray bars. Uninduced and induced control compounds without DMSO are on the left and with 0.1% DMSO on the right. Errors shown are the fractional standard deviation. (A) Expression of VEGF in cultured U251 cells under DFO-induced hypoxic conditions of match core control compounds **1−4** and mismatch core control compounds **12−15** at $1\,\mu$M concentration. Cells were treated with match compounds **6−8** and respective mismatch compounds **17−19** as 1, 0.2, and 0.02 μM cell culture media solutions. (B) Expression of VEGF in cultured LNCaP cells under DFO-induced hypoxic conditions of match core control compounds **1−4** and mismatch core control compounds **12−15** at 10 μM concentration. Cells were treated with match compounds **6−8** and respective mismatch compounds **17−19** as 10, 2, and 0.2 μM cell culture media solutions.

method for determining the rank-order of binding affinities, although a quantitative K_a value is not obtained. The 14-mer oligonucleotide sequences (Materials and Methods) are based on
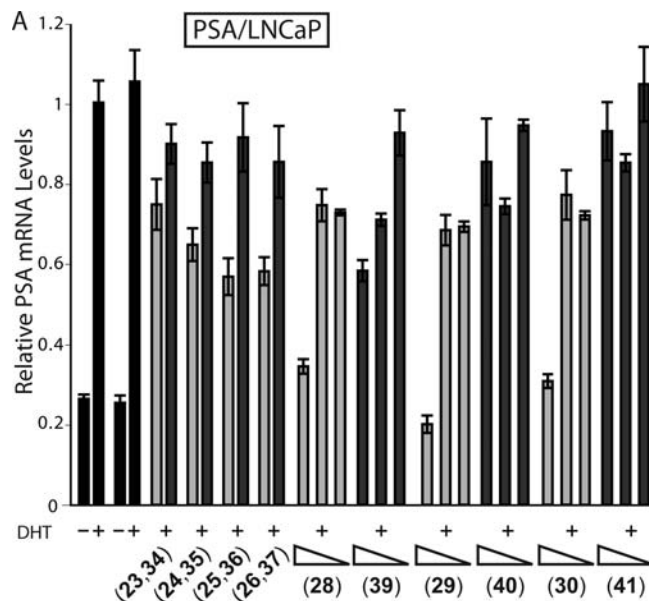

Figure 4. Quantitative real-time RT-PCR data measuring the effect on relative PSA mRNA expression levels under DHT induction in LNCaP cells dosed with compounds **23−26**, **28−30** and their mismatch congeners **34−37** and **39−41**. Induced and uninduced control conditions are indicated by black bars, match core compounds by light-gray bars, and mismatch core compounds by dark-gray bars. Uninduced and induced control compounds without DMSO are on the left and with 0.1% DMSO on the right. Errors shown are the fractional standard deviation. Cells were treated with match core control compounds **23−26** and mismatch core control compounds **34−37** as cell media solutions 5 μM in polyamide. Cells were treated with match compounds **28−30** and respective mismatch compounds **39−41** as 5, 1, and 0.1 μM solutions in cell culture media.

the HRE of VEGF and ARE of PSA, respectively. For both the HRE and ARE 14-mers, the melting temperature increased appreciably upon match compound binding (**1−11** and **23−33**, respectively). T_m values also generally increased upon mismatch binding (**12−22** and **34−44**, respectively) but to a more modest degree. Melting temperatures of the free amine parent compounds were higher than those of the IPA conjugates, with the exception of **36** versus **40**. The ΔT_m values calculated for match compounds ranged from an increase of 9.0 to 14.8 °C for the HRE polyamide series (**1−12**) and from an increase of 10.4 to 17.3 °C for the ARE series (**23−33**).

Cell Viability Effects of ARE-Targeted Match Compounds 28−33 and 39−44 in LNCaP Cells. LNCaP cells were dosed with each compound at concentrations spanning 30−0.01 μM, and metabolic activity was measured with a standard WST-1 colorimetric assay. Metabolic activity decreased with increasing concentrations of **28−30** but did not significantly surpass 50% viability; therefore, IC$_{50}$ values for growth inhibition could not be calculated. Cells treated with the mismatch mates (**39−41**) had little effect on cell growth. The three oxime-linked match compounds had measurable IC$_{50}$ values for growth inhibition: **31**, 1.7 $\pm$ (0.3) μM; **32**, 0.6 $\pm$ (0.1) μM; **33**, 0.4 $\pm$ (0.0) μM. The mismatch oximes displayed a similar pattern; the growth inhibition of the fluorine-bearing oximes **43** and **44** was more pronounced than the 3-carboxy tail mismatch **42**, but the effect on cell growth of the mismatch polyamides was less pronounced than that of the match polyamides. The cell growth data for **28−33** and **39−44** in LNCaP are shown in Figure 6 and Table 1.
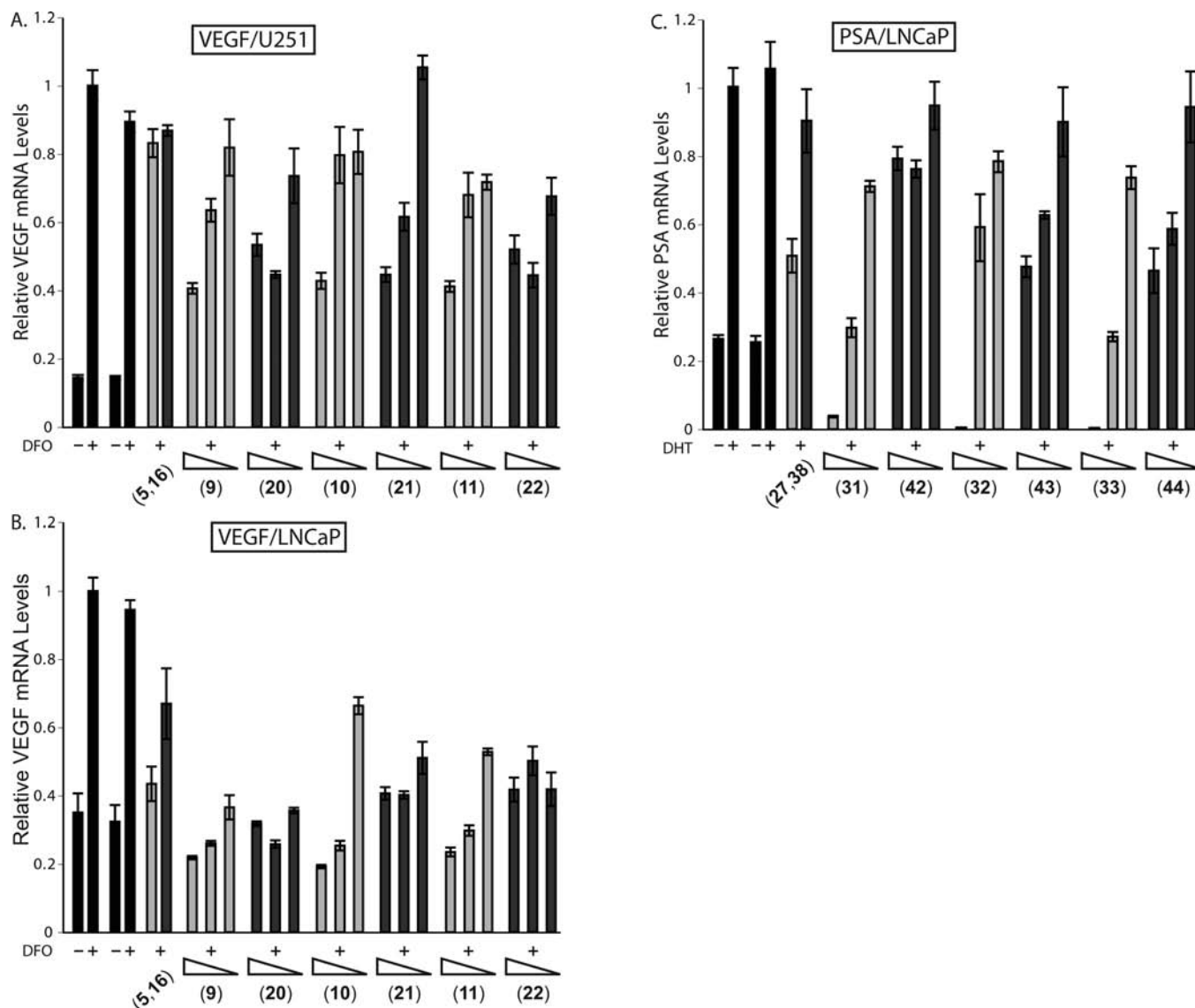
Figure 5. Gene-regulation effects measured by quantitative real-time RT-PCR for the oxime-linked polyamides **9−11**, **20−23**, **31−33**, and **42−44** and the hydroxylamine tail control compounds **5**, **16**, **27**, and **38**. Induced and uninduced control conditions are indicated by black bars, match core compounds by light-gray bars, and mismatch core compounds by dark-gray bars. Uninduced and induced control compounds without DMSO are on the left and with 0.1% DMSO on the right. Errors shown are the fractional standard deviation. (A) Effect on DFO-induced expression of VEGF by HRE-targeted match and mismatch polyamide cores in U251 cells at 1, 0.2, and 0.02 μM. (B) Effect on DFO-induced expression of VEGF by HRE-targeted match and mismatch polyamide cores in LNCaP cells at 10, 2, and 1 μM. (C) Effect on DHT-induced expression of PSA mRNA by ARE-targeted match and mismatch polyamide cores in LNCaP cells at 5, 1, and 0.1 μM.

Cell Viability Effects of Control Compounds 45−48 in U251 and LNCaP Cells. IC_{50} values for growth inhibition in U251 cells treated with oxime-linked polyamide coreless compounds **45−48** at a range of 10−0.002 μM and LNCaP cells at 50−0.02 μM were measured by a standard WST-1 colorimetric assay. Negligible cell viability effects were measured in either U251 or LNCaP cells after a 48 h treatment course with **45−48** at the concentrations used. These data are shown in Supporting Information Figure SI 2.

Gene Regulation IC_{50} Values for ARE-Targeted Oxime-Linked Compounds in LNCaP Cells. IC_{50} values for PSA mRNA expression levels were measured for **28**, **31**, and **33** by quantitative real-time RT-PCR in LNCaP cells. **28** was used as a benchmark, and **31** and **33** were selected on the basis of their high biological activity and to provide variety in the tail substitution. Cells were dosed with **28** at a range of 30−0.1 μM and **31** and **33** at 10−0.03 μM. Isotherms were generated for each of three independently performed real-time quantitative RT-PCR experiments in LNCaP cells for **28**, **31**, and **33**. An IC_{50} value was generated for each run, and the IC_{50} value given in Table 1 for each compound is the average value of three independent measurements (error given is the standard error of the mean (SEM) between the three independent runs). Isotherms (Figure 6B) were generated from the average value of the independent runs at each concentration (error bars are the SEM for each data point). Average IC_{50} values for gene regulation were as follows: **28**, 6.0 ($\pm$2.6) μM; **31**, 0.28 ($\pm$0.1) μM; **33**, 0.6 ($\pm$0.3) μM.

Discussion

A focused library of polyamides was synthesized with different modifications at the C-terminus, in which the linker, linkage, and tail group were varied and tested in two separate cell lines for gene regulation activity of two different target
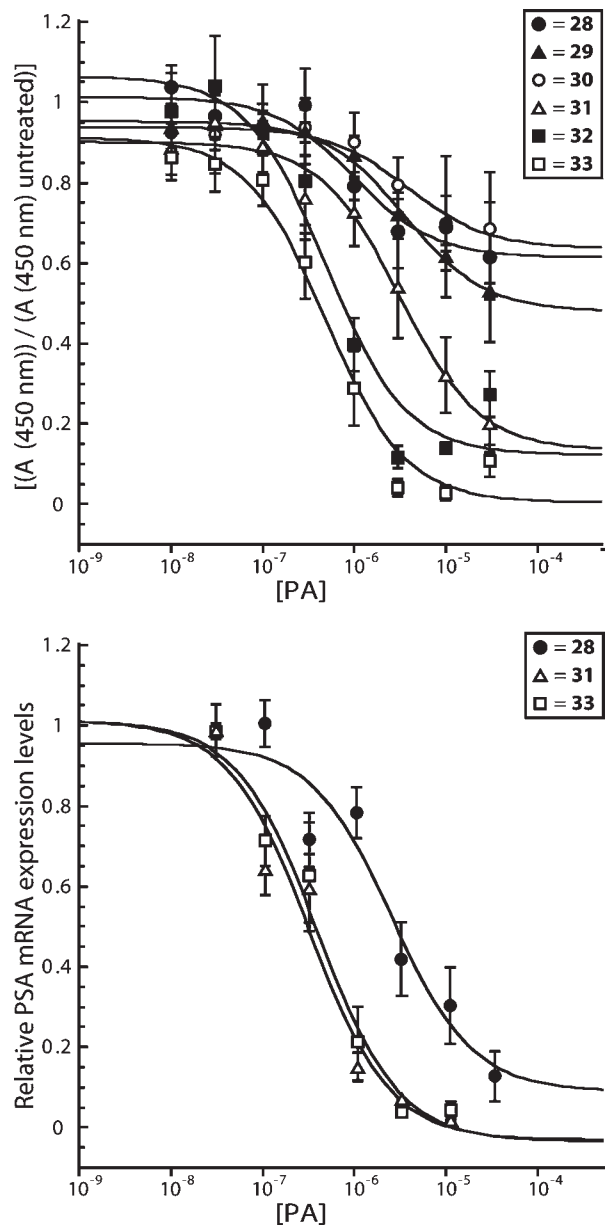
Figure 6. Cell viability data and IC$_{50}$ values for gene regulation for in LNCaP cell culture. (A, top) Cell viability was measured by a WST-1 colorimetric assay for LNCaP cells dosed for 48 h with polyamides **28**–**33** at the following concentrations: 30, 10, 3, 1, 0.3, 0.1, 0.03, and 0.01 μM. For **31**–**33**, IC$_{50}$ values for cell viability were extracted from isotherms generated in KaleidaGraph from the data. (B, bottom) Quantitative real-time RT-PCR data for **28**, **31** and **33** in LNCaP cells to establish IC$_{50}$ values for PSA regulation under inducing conditions. Concentrations employed for **28** were 30, 10, 3, 1, 0.3, and 0.1 μM, and for **31** and **33** they were 10, 3, 1, 0.3, 0.1, and 0.03 μM. IC$_{50}$ values were extracted from isotherms generated in Kaleidagraph from the RT-PCR titrations. (C) IC$_{50}$ values (μM) for cell viability estimated or calculated for **28**–**33**, and IC$_{50}$ values (μM) for PSA gene regulation for **28**, **31**, and **33** shown in tabular format. Values given are average values of three independent experiments; the standard error of the mean is given in parentheses.

genes. Prior to the current study, no direct comparison of the gene regulatory activity of a polyamide series between multiple cell lines had been performed. Measurement of VEGF mRNA expression levels in both U251 and LNCaP for the entire amide- and oxime-linked series was performed in an

effort to evaluate whether modifications in tail or linker structures can have differing effects on biological activity in a cell-line dependent fashion. The polyamide dose required to effect gene regulation activity was found to be cell-line dependent, but the trend in relative activities of polyamides did not vary greatly between different cell lines. Two encouraging results of this study were the degree to which changes in the linker composition are well tolerated and the significant increase in biological activity achieved upon replacement of an amide linkage with an oxime linkage between the linker and tail groups.

The biological activity of a series of polyamides targeted to the HRE of VEGF was measured under hypoxic (inducing) conditions in two different cell lines, U251 (glioma) and LNCaP (prostate cancer) lines. Polyamide regulation of DFO-induced VEGF expression in LNCaP cells has not previously been published. In the HRE-targeted amine series (**1**–**8** and **12**–**19**), a slight linker effect was observed but varied between the two cell lines. Overall, changes in the linker group did not dramatically affect biological activity in either cell line. The most pronounced effect was conjugation of the IPA tail, which resulted in an increase for each linker group in both cell lines, with the exception of the C3 linker in LNCaP cells. IPA conjugation affected biological activity of the triamine-linked compounds most significantly in both U251 and LNCaP.

The amide-linked ARE series was assayed for activity against DHT-induced, AR-regulated PSA expression in LNCaP cells. Removal of the tertiary amine in the linker resulted in an increase in biological activity, as seen for **29** vs **28**, while reduction in linker length from a C7 to a C3 linker led to a modest loss of activity (**29** vs **30**). Although the mechanism by which mismatch polyamides affect gene expression is unknown, removal of the tertiary amine reduces mismatch activity (e.g., **39** is more active than **40** and **41**). These results again indicate that there is tolerance of linker group modification and that the ARE system in LNCaP cells benefits from removal of the amine group in the linker. The T_m data indicate that the absence of biological activity is not due to an inability of the polyamides to bind to DNA, as each of the IPA conjugates has a lower T_m than their respective free-amine parent compounds but higher biological activity. The triamine-bearing polyamides **24** and **28**, in fact, have higher T_m values than the neutral, aliphatic linker-bearing polyamides **25** and **29** (C7 linker) and **26** and **30** (C3 linker) (free amine and IPA, respectively, for each pair). These data suggest that the presence of the tertiary amine and the positive charge increase the binding affinity of these polyamides.

Oxime-linked polyamides were synthesized for both the HRE (**9**–**11**, **20**–**22**) and ARE (**31**–**33**, **42**–**44**) systems. The oxime had been introduced as an efficient means of conjugating a polyamide core to ^{18}F-labeled 4-fluorobenzaldehyde for PET studies, but the ability of polyamides possessing this motif to regulate endogenous gene expression was not known. The aldehyde tail groups selected were 4-fluorobenzaldehyde, 3-fluorobenzaldehyde, and 3-carboxybenzaldehyde; 3-fluorobenzaldehyde was selected to probe position effects, and 3-carboxybenzaldehyde provided an oxime-linked mimic of the amide-linked IPA tail.

In U251 cells (Figure 5A), the oxime linked match (**9**–**11**) polyamides had activity comparable to the triamine- or C7-linker amide-linked IPA conjugates (**6** and **7**, respectively). Introduction of the oxime linker had a more significant impact on the biological activity of the mismatch polyamides **20**–**22**, which were as active as their oxime-linked counterparts **9**–**11**.

Table 1. Table of IC$_{50}$ Values (μM) for Growth Inhibition and Gene Regulation in LNCaP Cells for **28**–**33**[a]

compd	IC$_{50}$ (μM)		(growth inhibition IC$_{50}$ (μM))/(gene regulation IC$_{50}$ (μM))
	growth inhibition	gene regulation	
28	> 30	6.0 ± 2.6	≥ 5
29	> 30		
30	> 30		
31	1.7 ± 0.3	0.3 ± 0.1	6.1
32	0.6 ± 0.1		
33	0.4 ± 0.0	0.6 ± 0.3	0.7

[a] Data are shown in Figure 5. IC$_{50}$ for gene regulation was measured only for **28**, **31**, and **33**. For **28**, **31**, and **33**, the (IC$_{50}$ for growth inhibition)/(IC$_{50}$ for gene regulation) ratio was calculated.

A similar result was seen for the C7- and C3-linker, amide-linked IPA conjugate pairs **7** and **18**, and **8** and **19**, in U251 cells. Thus, although there does appear to be tolerance of linker variations, the greatest difference in biological activity within an HRE match–mismatch pair in U251 cells is the triamine-linked IPA compounds **6** and **17**.

In LNCaP cells (Figure 5B), the HRE-oxime series **9**–**11** were more active than the amide-linked series **6**–**8** and in fact reduced VEGF mRNA expression levels to below baseline levels. In this case, introduction of fluorine on the tail restored the match–mismatch activity difference to ~2-fold (i.e., **9** and **20**, or **10** and **21**, or **11** and **22**). The T_m data for the oxime-linked polyamides and their parent unconjugated polyamides do not indicate that differences in binding affinity play any role in the differences in activity; the T_m values measured for the amide series, both match and mismatch cores, are comparable to those measured for the oxime series.

Polyamide regulation of VEGF expression in LNCaP had not been studied, but it was known that polyamide-effected regulation of PSA in LNCaP cells can be achieved with 10 and 5 μM **28**. A 10-fold higher concentration of HRE polyamides was required in LNCaP cells compared to U251 cells to effect comparable VEGF gene regulation. Although the effects on VEGF expression in LNCaP and U251 cells of the HRE polyamide series vary somewhat, it is encouraging that there are no drastic differences in biological activity measured for any of the compounds tested between the two cell lines. This suggests that a structural modification that results in increased gene regulation in one cell line may have a similar effect for the same core in other cell lines.

The data for the oxime-linked ARE series (**31**–**33**, **42**–**44**) in LNCaP cells (Figure 5C) indicate that the oxime linkage greatly increases the gene regulation activity of the ARE polyamides. PSA mRNA expression was negligible in cells treated with **31**–**33** at 5 μM, but there was evidence of cell death upon visual inspection (vide infra) and levels of total mRNA were very low. The average gene expression titration curve generated by quantitative real-time RT-PCR for **28**, **31**, and **33** is shown in Figure 6B. These data illustrate the impact of the oxime linkage on the biological activity, as the activity curves of the oxime compounds **31** and **33** are shifted down by a factor of ≥10-fold from the amide-linked triamine IPA parent polyamide **28** (IC$_{50}$ values in Table 1).

To quantitate the effect of **28**–**33** and **39**–**44** on cell growth in LNCaP cells, cells were treated with compounds and viability was measured (Figure 6A (**28**–**33**) and Figure SI 1 (**39**–**44**)). Cells treated with the amide-linked compounds at

these concentrations did not show ≥50% decrease in cell growth, so an IC$_{50}$ value for growth inhibition could not be calculated. IC$_{50}$ values for growth inhibition were calculated for **31**–**33** (Table 1). Oxime mismatch polyamide **42** minimally affected cell viability, while **43** and **44** had estimated IC$_{50}$ values for cell viability of ≥30 μM. The IC$_{50}$ values for gene regulation for **31** and **33** are 20- and 10-fold lower than **28**, respectively. In the case of the 4-fluorooxime-linked compound **33**, the IC$_{50}$ values for growth inhibition and gene regulation are within error of each other. The IC$_{50}$ for growth inhibition of **28** and **31** is ~5-fold higher than the IC$_{50}$ for gene regulation, but both these values are ~20-fold lower for **31** than for **28**, indicating that **31** is ~20-fold more potent than **28** and more specific than **33**.

These results indicate that the oxime linkage can effect a significant increase in the cell uptake and gene regulation activity of polyamides. For unconjugated hydroxylamine polyamides **27** and **38**, a ~50% and 10% down-regulation was measured, respectively, of induced PSA mRNA expression in LNCaP cells at 5 μM, and **27** and **38** were significantly less active than the oxime conjugates. Although previous studies have rigorously verified the stability of oxime-linked conjugates in vivo, a control experiment was performed where polyamide-lacking compounds **45**–**48** were synthesized and their cytotoxicity measured.[19] It was rationalized that cytotoxicity equivalent to that of oxime polyamide conjugates would serve as an indirect measure of bond lability, whereas a lack to toxicity would reinforce the robustness of this chemical bond. The growth inhibitory effects of these compounds were studied in U251 and LNCaP cells (parts A and B of Figure SI 2, respectively). Treatment with **45**–**48** in both cells lines failed to cause dramatic cell death at any concentrations used (10–0.002 μM in U251, 50–0.02 μM in LNCaP), indicating that the oxime linkage did not decompose and invoke cell death. These results suggest that the oxime linkage is promising for future work aimed at increasing polyamide potency.

Although not the focus of the current study, the mechanisms of polyamide cell entry, nuclear localization, and cell exit are active areas of investigation.[11] Our current working hypothesis for polyamide biological activity is that passive or nonspecific mechanisms of polyamide cell uptake and competing efflux pathways influence polyamide accumulation in the cell nucleus, and structural modifications that result in improved polyamide biological activity may reflect a decrease in efflux. Polyamides are believed in part to undergo active efflux by p-glycoprotein pumps, which have more pronounced activity in immortalized cancer cells such as those employed in the current study.[20,21] The chemical agent verapamil, which inhibits p-glycoprotein pump activity, has been found to result in nuclear localization for some fluorophore–polyamide conjugates.[10] The mechanistic basis for the improved activity observed upon introduction of structural features such as the IPA tail is unknown, but we speculate that it is partially due to reduced polyamide efflux.

The tolerance of modifications to the linker group suggests that further modifications to the linker group may lead to improved polyamide biological activity. Comparison of the data gathered for the HRE match and mismatch polyamides in U251 and LNCaP cells indicate that while the concentrations required to achieve acceptable levels of gene regulation activity will vary between cell lines, the effect of structural modifications will most likely be comparable between cell lines; i.e., the trends in activity will translate between cell lines. In addition, the use of an oxime linkage in place of an amide

linkage between the tail and linker groups was found to increase the gene regulation activity of polyamides. This increase was most noticeable for the ARE oxime-linked series **31**−**33** in LNCaP cells. The dramatic increase in activity measured for **31** compared to the previously published results for **28** makes this compound and related derivatives useful for future ARE studies. In addition, these results suggest that the oxime linkage may be a useful structural feature to increase the biological activity of polyamides in other biological studies. Although this study did not uncover a set of predictive structural requirements for polyamide cell uptake, the discovery of the utility of the oxime linkage for gene regulation studies is a welcome addition to the known set of structural modifications to increase polyamide cell uptake.

Materials and Methods

Synthesis of Polyamides. Polyamides were synthesized by solid-phase methods on Kaiser oxime resin (NovaBiochem) or Boc-β-alanine-PAM resin (Peptides International), were cleaved from resin with 3,3′-diamino-N-methyl-dipropylamine, N,N'-dimethylpropane-1,3-diamine (Dp), heptane-1,7-diamine, propane-1,3-diamine, or *tert*-butyl 3-aminopropoxycarbamate, and purified by reverse-phase HPLC.[16,22−24] Synthesis of IPA conjugates and oxime conjugates was as previously described.[8,16] Reaction progress was monitored by analytical HPLC at 310 nm. Turn deprotection was done through addition of 1 mL of 1:1 TFA/DCM at ambient temperature, and purification by reverse-phase preparative HPLC was performed immediately following successful deprotection. Reverse-phase HPLC solvent systems were 0.1% TFA (aqueous) and acetonitrile. Polyamide purity and identity were assessed by analytical HPLC (310 nm) and MALDI-ToF MS, and polyamides were quantitated by UV−vis at 310 nm ($\varepsilon = 69\,360$ M^{-1} cm^{-1} for eight-ring hairpin polyamides). Purity of all compounds was ≥95% by analytical HPLC. Supporting Information Table SI 1 provides expected and observed (M+H$^+$) (MALDI-ToF MS) and purity by analytical HPLC for **1**−**44**. ^{1}H and ^{13}C NMR spectra were obtained on a 500 MHz spectrometer.

Synthesis of 45. An amount of 1 equiv (84.3 mg, 0.44 mmol) of *tert*-butyl 3-(aminooxy)propylcarbamate was dissolved in 300 μL of DMF, and 1.2 equiv of 3-formylbenzoic acid added as a 50 mM solution in DMF.[25] Reaction progress was monitored by analytical HPLC at 254 nm for starting material consumption and production of a mixture of the *E*- and *Z*-3-(10,10-dimethyl-8-oxo-3,9-dioxa-2,7-diazaundec-1-enyl)benzoic acid intermediate. Upon consumption of starting material, the Boc protecting group was removed by addition of 4 mL of 1:1 TFA/ DCM. After 15 min, the mixture was concentrated by rotovap and the product purified by reverse phase preparatory HPLC. The *E* and *Z* products were separable by preparative HPLC but interconvert at room temperature on the time-scale of the experiments and so were recombined to yield 43.3 mg (44% yield) of 3-((3-aminopropoxyimino)methyl)benzoic acid (**45**). ^{1}H NMR (DMSO-d_6): δ 13.23 (s, 1H), 8.36 (s, 1H), 8.20 (app t, $J = 1.8$ Hz, 1H), 7.96 (app dt, 7.8, 1.8, 1 Hz, 1H), 7.88 (br s, 3H), 7.84 (app dt, 8.0, 1.5 Hz, 1H), 7.55 (app t, 7.8 Hz, 1H), 4.20 (t, 6.3 Hz, 2H), 2.91 (t, 7.3 Hz, 2H), 1.96 (m, 2H). ^{13}C NMR (DMSO-d_6): δ 166.8, 148.6, 132.3, 131.4, 131.0, 130.6, 129.2, 127.4, 70.6, 36.2, 27.0. Exact mass (M + H$^+$): calcd, 223.1083; found, 223.1078.

Synthesis of 46. An amount of 1 equiv (83.8 mg, 0.44 mmol) of *tert*-butyl 3-(aminooxy)propylcarbamate was used to synthesize **45**, as above. Following Boc deprotection and prior to purification, 2 equiv of (Ac)$_2$O (83.2 μL, 0.88 mmol) and 2.5 equiv of DIEA (191.6 μL, 1.1 mmol) were added. Reaction progress was monitored by analytical HPLC at 254 nm, and the product was purified by preparative reverse phase HPLC. As above, the *E* and *Z* enantiomers were separable but were recombined to yield

108.3 mg (93% yield) of the 3-((3-acetamidopropoxyimino)-methyl)benzoic acid product **46**. ^{1}H NMR (DMSO-d_6): δ 13.14 (s, 1H), 8.33 (s, 1H), 8.18 (t, 1.8 Hz, 1H), 7.95 (app dt, 7.5, 1.5 Hz, 1H), 7.87 (br t, 4.8 Hz, 1H), 7.83 (app dt, 8.3, 1.5 Hz, 1H), 7.54 (app t, 7.8 Hz, 1H), 4.14 (t, 6.5 Hz, 2H), 3.12 (m, 2H), 1.79 (s, 3H), 1.78 (m, 2H). ^{13}C NMR (DMSO-d_6): δ 169.1, 166.8, 148.0, 132.5, 131.3, 130.9, 130.4, 129.2, 127.4, 71.5, 35.4, 28.9, 22.6. Exact mass (M + H$^+$): calcd, 265.1188; found, 265.1199.

Synthesis of 47. The synthesis and purification of **47** proceeded as described for **45** but with 4-fluorobenzaldehyde. Yield: 66.8 mg (74%). ^{1}H NMR (DMSO-d_6): δ 8.27 (s, 1H), 7.86 (br s, 3H), 7.66 (m, 2H), 7.26 (m, 2H), 4.17 (t, 6.3 Hz, 2H), 2.90 (m, 2H), 1.94 (m, 2H). ^{13}C NMR (DMSO-d_6): δ 164.0, 162.0, 129.0 ($J = 28$ Hz), 128.5 ($J = 11$ Hz), 115.9 ($J = 86$ Hz), 70.4, 36.2, 27.0. Exact mass (M + H$^+$): calcd, 197.1090; found, 197.1091.

Synthesis of 48. The synthesis and purification of **48** proceeded as described for **46** but with 4-fluorobenzaldehyde. Yield: 103.3 mg (89%). ^{1}H NMR (DMSO-d_6): δ 8.24 (s, 1H), 7.87 (br s, 1H), 7.65 (m, 2H), 7.24 (m, 2H), 4.10 (t, 6.5 Hz, 2H), 3.11 (m, 2H), 1.78 (s, 3H), 1.76 (m, 2H). ^{13}C NMR (DMSO-d_6): δ 169.1, 164.0, 162.0, 129.0 ($J = 33$ Hz), 128.6 ($J = 13$ Hz), 115.8 ($J = 87.5$ Hz), 71.3, 35.5, 28.9, 22.6. Exact mass (M + H$^+$): calcd, 239.1196; found, 239.1189.

Determination of DNA Melting Temperature (T_m) Values. Melting temperatures were measured according to a previously published methodology on a Varian Cary 100 spectrophotometer equipped with a thermocontrolled cuvette holder and quartz cuvettes (1 cm path length).[18] The buffer was an aqueous solution of 10 mM sodium cacodylate, 10 mM KCl, 10 mM MgCl$_2$, and 5 mM CaCl$_2$ at pH 7.0. Oligonucleotide sequences were 5′-GTGCATACGTGGGC-3′ (HRE 14-mer top), 5′-GCCCACGTATGCAC-3′ (HRE 14-mer bottom), 5′-TTGCA-GAACAGCAA-3′ (ARE 14-mer top), and 5′-TTGCTGTT-CTGCAA-3′ (ARE 14-mer bottom).

Cell Culture Experiments. For cell culture experiments, a polyamide stock solution in DMSO and DNase/RNase-free water was prepared by dissolving 5−30 nmol of polyamide in DMSO (1−3 μL), followed by addition of DNase/RNase-free water to a target concentration of 50 M. Suspensions were centrifugated to remove undissolved material, and solution concentration was determined by UV−vis measurement of a 100× diluted solution at 310 nm ($\varepsilon = 69\,360$ M^{-1} cm^{-1} for eight-ring hairpin polyamides). The DMSO concentration of cell media solutions was kept below 0.1%, and a DMSO control was included in quantitative real-time RT-PCR (see below).[17] Isotherms were generated using the following modified Hill equation: $Y = m_1 + (m_2 - m_1)/(1 + (m_0/m_3))$, where $m_1 = 100$, $m_2 = 5000$, $m_3 = 5\,e^{-7}$.

Measurement of Cell Viability in U251 and LNCaP Cells. U251 and LNCaP cells were maintained as previously described.[8,14] For the growth inhibition assay, cells were plated in 96-well plates in 0.2 mL at $(10−15) \times 10^2$ cells per well $((15−20) \times 10^3$ cells/mL). After 24 h (U251) or 48 h (LNCaP), 150 μL of medium was removed and replaced with 50 μL of 2× (polyamide concentration) cell medium solutions. After 48 h, the medium was replaced with 100 μL of fresh medium, and cells were allowed to recover for 24 h before addition of 10 μL of WST-1 reagent (Roche) to each well. Cells were incubated for 30 min, and absorbance at 450 nm was measured. Untreated controls and cell-free, media-only controls were included on each plate, and each well was corrected for average background absorption of media-only controls before normalization of the average absorption for each concentration to untreated controls.

Measurement of Induced Gene Expression in U251 and LNCaP Cells. Measurement of hypoxia-induced VEGF expression in U251 cells and DHT-induced PSA expression in LNCaP cells was as previously described.[8,14] Measurement of hypoxia-induced VEGF expression in LNCaP cells followed the protocol for DHT-induced PSA expression in LNCaP cells but with the

following changes: gene induction was by DFO, and FBS (not charcoal stripped) was used. Primer sequences were as follows: VEGF, L 5′-AGGGCAGAATCATCACGAAG-3′, R 5′-GGGTACTCCTGGAAGATGTCC-3′; PSA, L 5′-TCTG-CGGCGGTGTTCTG-3′, R 5′-GCCGACCCAGCAAGATC-A-3′; β-glucuronidase, L 5′-CTCATTTGGAATTTTGCCG-ATT-3′, R 5′-CCGAGTGAAGATCCCCTTTTTA-3′.

Supporting Information Available: MALDI-ToF and purity by analytical HPLC data for **1**−**44**, T_m data for **1**−**44**, cell viability data for **39**−**44** in LNCaP cells, and cell viability data for **45**−**48** in LNCaP and U251 cells. This material is available free of charge via the Internet at http://pubs.acs.org.

References

(1) Brennan, P.; Donev, R.; Hewamana, S. Targeting transcription factors for therapeutic benefit. *Mol. BioSyst.* **2008**, *4*, 909–919.
(2) Berg, T. Inhibition of transcription factors with small organic molecules. *Curr. Opin. Chem. Biol.* **2008**, *12*, 464–471.
(3) Dervan, P. B.; Edelson, B. S. Recognition of the DNA minor groove by pyrrole−imidazole polyamides. *Curr. Opin. Struct. Biol.* **2003**, *13*, 284–299.
(4) White, S.; Szewczyk, J. W.; Turner, J. M.; Baird, E. E.; Dervan, P. B. Recognition of the four Watson−Crick base pairs in the DNA minor groove by synthetic ligands. *Nature* **1998**, *391*, 468–471.
(5) Kielkopf, C. L.; Baird, E. E.; Dervan, P. B.; Rees, D. C. Structural basis for G.C recognition in the DNA minor groove. *Nat. Struct. Biol.* **1998**, *5*, 104–109.
(6) Foister, S.; Marques, M. A.; Doss, R. M.; Dervan, P. B. Shape selective recognition of T/A base pairs by hairpin polyamides containing N-terminal 3-methoxy (and 3-chloro) thiophene residues. *Bioorg. Med. Chem.* **2003**, *11*, 4333–4340.
(7) Hsu, C. F.; Phillips, J. W.; Trauger, J. W.; Farkas, M. E.; Belitsky, J. M.; Heckel, A.; Olenyuk, B. Z.; Puckett, J. W.; Wang, C. C.; Dervan, P. B. Completion of a programmable DNA-binding small molecule library. *Tetrahedron* **2007**, *63*, 6146–6151.
(8) Nickols, N. G.; Jacobs, C. S.; Farkas, M. E.; Dervan, P. B. Improved nuclear localization of DNA-binding polyamides. *Nucleic Acids Res.* **2007**, *35*, 363–370.
(9) Belitsky, J. M.; Leslie, S. J.; Arora, P. S.; Beerman, T. A.; Dervan, P. B. Cellular uptake of *N*-methylpyrrole/*N*-methylimidazole polyamide−dye conjugates. *Bioorg. Med. Chem.* **2002**, *10*, 3313–3318.
(10) Crowley, K. S.; Phillion, D. P.; Woodard, S. S.; Schweitzer, B. A.; Singh, M.; Shabany, H.; Burnette, B.; Hippenmeyer, P.; Heitmeier, M.; Bashkin, J. K. Controlling the intracellular localization of fluorescent polyamide analogues in cultured cells. *Bioorg. Med. Chem. Lett.* **2003**, *13*, 1565–1570.
(11) Best, T. P.; Edelson, B. S.; Nickols, N. G.; Dervan, P. B. Nuclear localization of pyrrole−imidazole polyamide−fluorescein conjugates in cell culture. *Proc. Natl. Acad. Sci. U.S.A.* **2003**, *100*, 12063–12068.
(12) Edelson, B. S.; Best, T. P.; Olenyuk, B.; Nickols, N. G.; Doss, R. M.; Foister, S.; Heckel, A.; Dervan, P. B. Influence of structural variation on nuclear localization of DNA-binding polyamide−fluorophore conjugates. *Nucleic Acids Res.* **2004**, *32*, 2802–2818.
(13) Olenyuk, B. Z.; Zhang, G. J.; Klco, J. M.; Nickols, N. G.; Kaelin, W. G.Jr.; Dervan, P. B. Inhibition of vascular endothelial growth factor with a sequence-specific hypoxia response element antagonist. *Proc. Natl. Acad. Sci. U.S.A.* **2004**, *101*, 16768–16773.
(14) Nickols, N. G.; Dervan, P. B. Suppression of androgen receptor-mediated gene expression by a sequence-specific DNA-binding polyamide. *Proc. Natl. Acad. Sci. U.S.A.* **2007**, *104*, 10418–10423.
(15) Nickols, N. G.; Jacobs, C. S.; Farkas, M. E.; Dervan, P. B. Modulating hypoxia-inducible transcription by disrupting the HIF-1-DNA interface. *ACS Chem. Biol.* **2007**, *2*, 561–571.
(16) Harki, D. A.; Satyamurthy, N.; Stout, D. B.; Phelps, M. E.; Dervan, P. B. In vivo imaging of pyrrole−imidazole polyamides with positron emission tomography. *Proc. Natl. Acad. Sci. U.S.A.* **2008**, *105*, 13039–13044.
(17) Tjernberg, A.; Markova, N.; Griffiths, W. J.; Hallen, D. DMSO-related effects in protein characterization. *J. Biomol. Screening* **2006**, *11*, 131–137.
(18) Dose, C.; Farkas, M. E.; Chenoweth, D. M.; Dervan, P. B. Next generation hairpin polyamides with (*R*)-3,4-diaminobutyric acid turn unit. *J. Am. Chem. Soc.* **2008**, *130*, 6859–6866.
(19) Kalia, J.; Raines, R. T. Hydrolytic stability of hydrazones and oximes. *Angew. Chem., Int. Ed.* **2008**, *47*, 7523–7526.
(20) Juliano, R. L.; Ling, V. A surface glycoprotein modulating drug permeability in Chinese hamster ovary cell mutants. *Biochim. Biophys. Acta* **1976**, *455*, 152–162.
(21) Ueda, K.; Cardarelli, C.; Gottesman, M. M.; Pastan, I. Expression of a full-length cDNA for the human "MDR1" gene confers resistance to colchicine, doxorubicin, and vinblastine. *Proc. Natl. Acad. Sci. U.S.A.* **1987**, *84*, 3004–3008.
(22) Belitsky, J. M.; Nguyen, D. H.; Wurtz, N. R.; Dervan, P. B. Solid-phase synthesis of DNA binding polyamides on oxime resin. *Bioorg. Med. Chem.* **2002**, *10*, 2767–2774.
(23) Baird, E. E.; Dervan, P. B. Solid phase synthesis of polyamides containing imidazole and pyrrole amino acids. *J. Am. Chem. Soc.* **1996**, *118*, 6141–6146.
(24) Salisbury, C. M.; Maly, D. J.; Ellman, J. A. Peptide microarrays for the determination of protease substrate specificity. *J. Am. Chem. Soc.* **2002**, *124*, 14868–14870.
(25) Wallace, E.; Hurley, B.; Yang, H.; Lyssikatos, J.; Blake, J.; Marlow, A. Heterocyclic Inhibitors of MEK and Methods of Use Thereof. U.S. Patent Application 20050054701 A1, 2005.